

Supplementary Materials for

Chronic Activation of mTOR Complex 1 Is Sufficient to Cause Hepatocellular Carcinoma in Mice

Suchithra Menon, Jessica L. Yecies, Hui H. Zhang, Jessica J. Howell, Justin Nicholatos, Eylul Harputlugil, Roderick T. Bronson, David J. Kwiatkowski, Brendan D. Manning*

*To whom correspondence should be addressed. E-mail: bmanning@hsph.harvard.edu

Published 27 March 2012, *Sci. Signal.* **5**, ra24 (2012)

DOI: 10.1126/scisignal.2002739

The PDF file includes:

Fig. S1. mTORC1 signaling is increased in the livers of obese mice, and *LTscIKO* mice exhibit sustained mTORC1 signaling under fasting conditions.

Fig. S2. *LTscIKO* female mice also develop HCC.

Fig. S3. *LTscIKO* mice are protected from age-related hepatic steatosis.

Fig. S4. Status of pathways that contribute to HCC and metabolic proteins in normal and tumor tissue of *LTscIKO* livers.

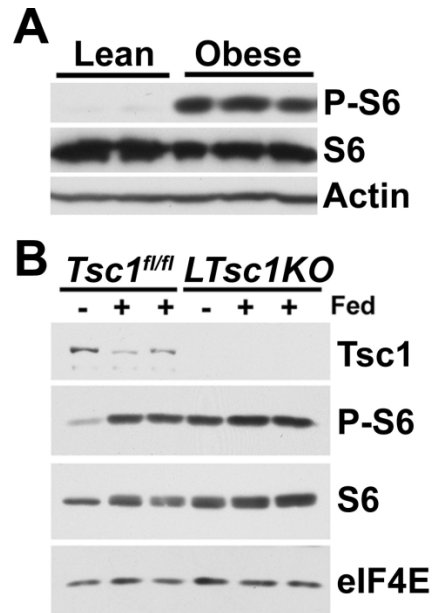
Fig. S5. Changes in *LTscIKO* livers at 6 months of age before the appearance of tumors.

Fig. S6. Long-term rapamycin treatment of *LTscIKO* mice decreases mTORC1 signaling, proliferation, apoptosis, inflammation, progenitor cell expansion, and DNA damage in the liver.

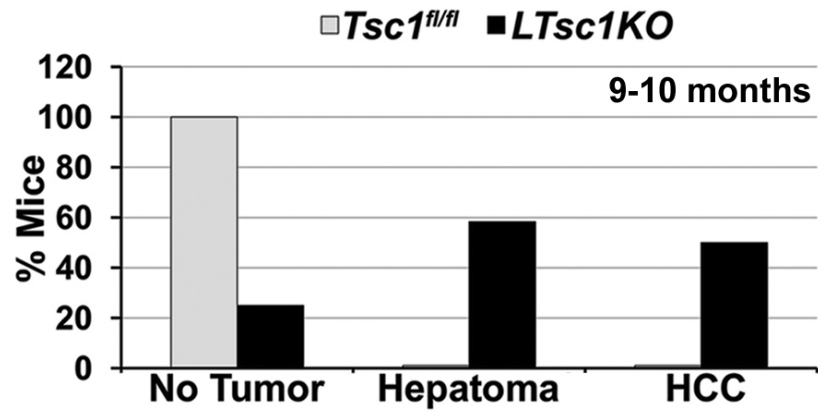
Fig. S7. Cytostatic, but not cytotoxic, response of *LTscIKO* liver tumors to rapamycin and inhibition of mTORC1 signaling by rapamycin in tumor regions resistant to rapamycin.

Fig. S8. ER stress and defective mitochondria in *LTscIKO* livers before the appearance of tumors.

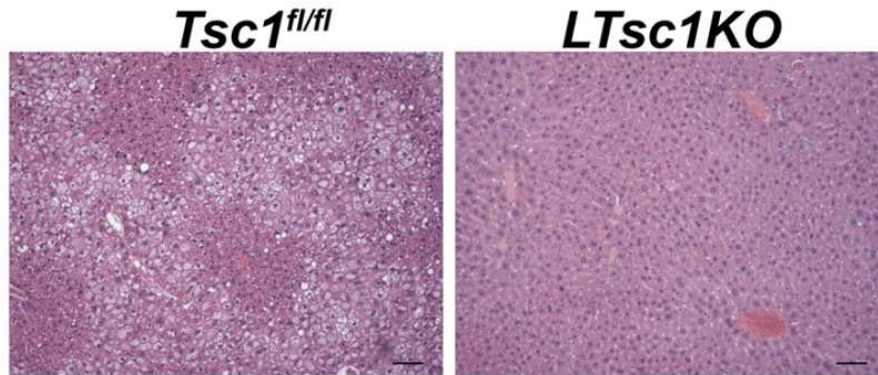
Table S1. RT-PCR primers used in this study.



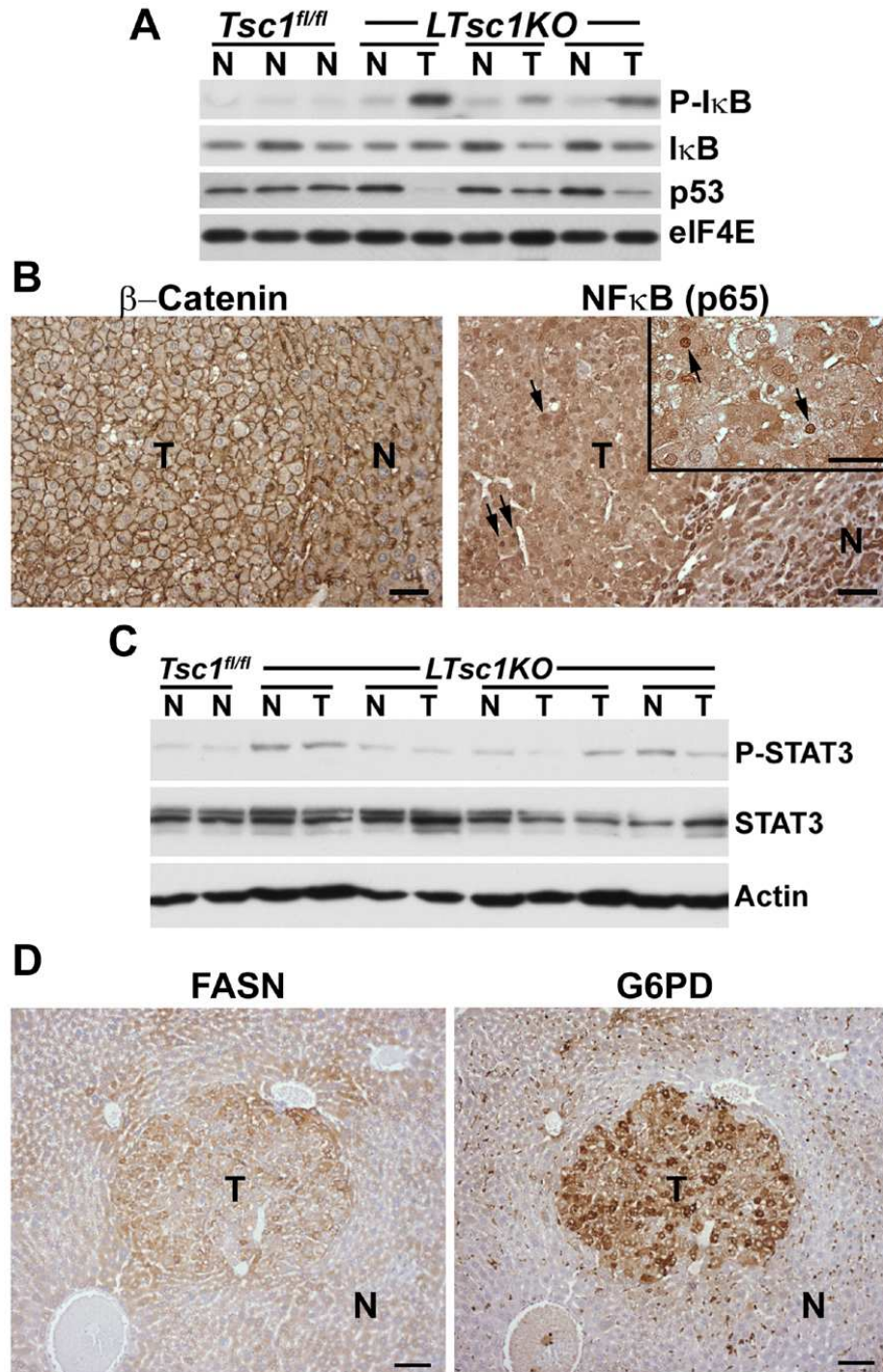
Supplemental Figure 1. mTORC1 signaling is increased in the livers of obese mice, and *LTsc1KO* mice exhibit sustained mTORC1 signaling under fasting conditions. **(A)** mTORC1 signaling is increased in the livers of obese mice. Immunoblot analysis of liver lysates from wild-type C57/BL6 mice (6 months) fed either a normal chow diet (lean) or high fat diet for the final 16 weeks (obese). **(B)** *LTsc1KO* mice exhibit sustained mTORC1 signaling under fasting conditions that is similar to the extent obtained in *Tsc1^{fl/fl}* mice just after feeding. Immunoblots of liver lysates from 3 month-old *Tsc1^{fl/fl}* and *LTsc1KO* mice that were fasted overnight and then re-fed for 1 hour (+), where indicated. Phospho-specific antibodies: S6 (Ser^{240/244}).



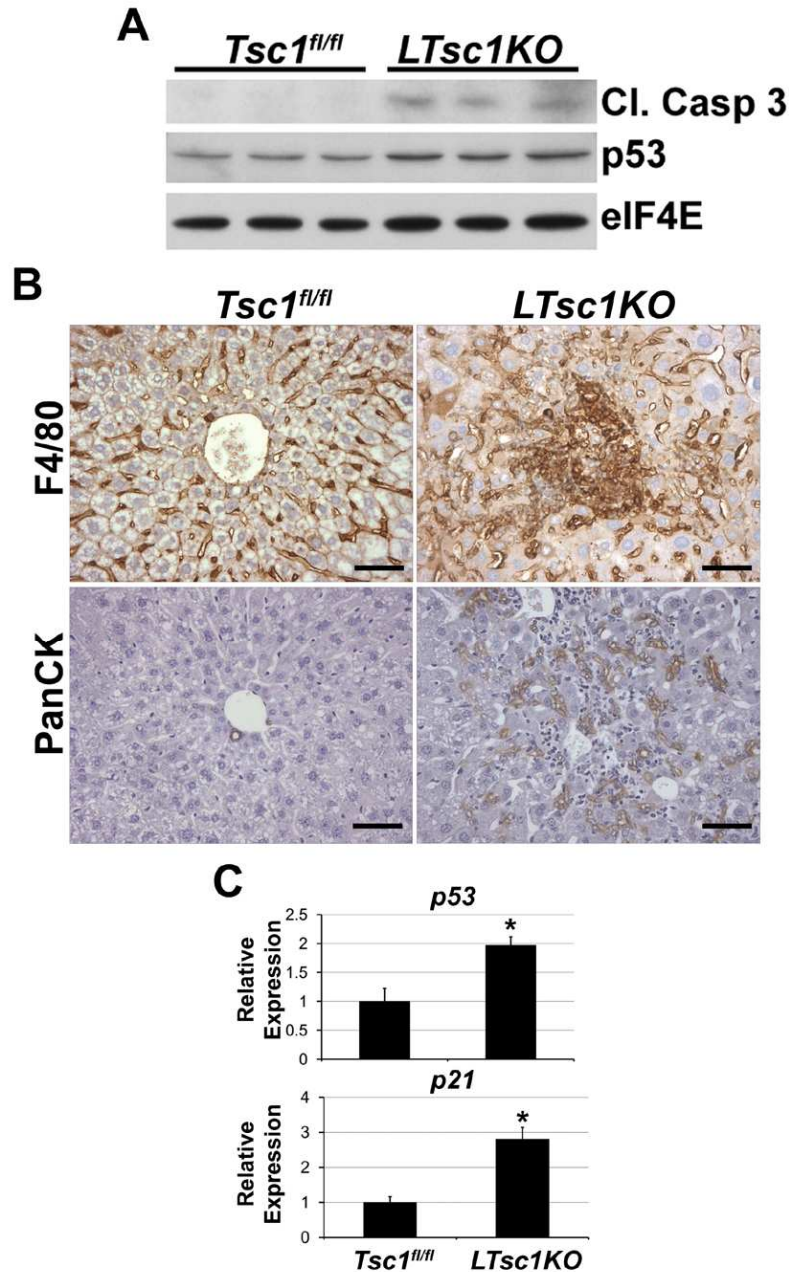
Supplemental Figure 2. *LTsc1KO* female mice also develop HCC. Percentage of *Tsc1^{fl/fl}* (n=9) and *LTsc1KO* (n=12) female mice with hepatomas (or nodular foci) and HCC at 9-10 months of age. One 4- μ m H&E-stained liver section per mouse was scored.



Supplemental Figure 3. *LTsc1KO* mice are protected from age-related hepatic steatosis. Representative H&E-stained sections of livers from *Tsc1^{fl/fl}* and *LTsc1KO* mice on a normal chow diet at 9 months of age are shown. Scale bar, 100 μm (100X).

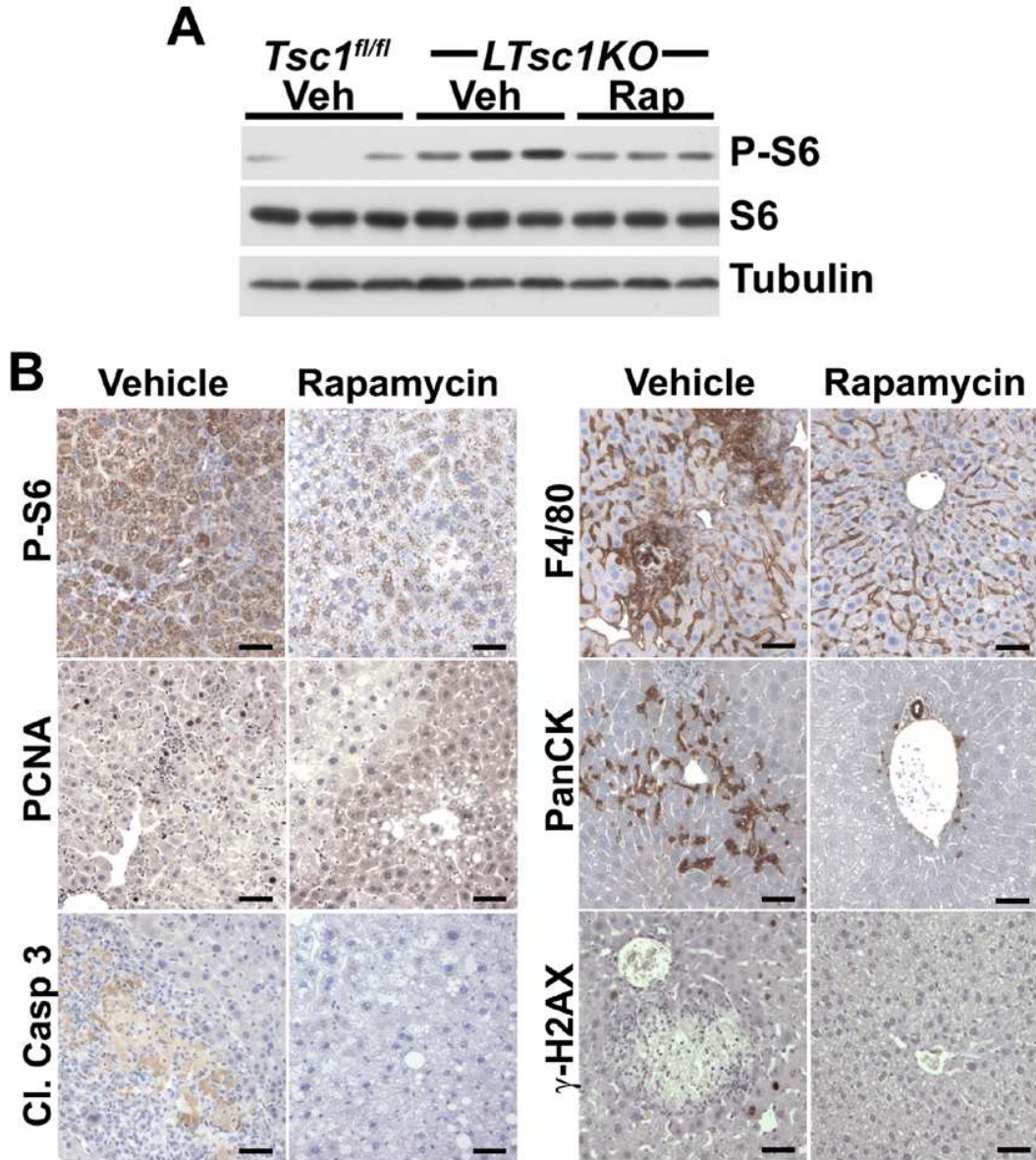


Supplemental Figure 4. Status of pathways that contribute to HCC and metabolic proteins in normal and tumor tissue of *LTsc1KO* livers. (**A,C**) Immunoblot analysis of liver lysates from non-tumor (N) or tumor (T) regions of *Tsc1^{fl/fl}* and *LTsc1KO* mice with the indicated antibodies. Phospho-specific antibodies: I κ B (Ser³²), STAT3 (Tyr⁷⁰⁵). (**B,D**) Representative immunohistochemical staining of liver sections from *Tsc1^{fl/fl}* and *LTsc1KO* mice with the indicated antibodies. Arrows indicate cells with nuclear accumulation of NF- κ B. Scale bars, **B**, 50 μ m (200X), inset 50 μ m (400X), **D**, 100 μ m (100X).



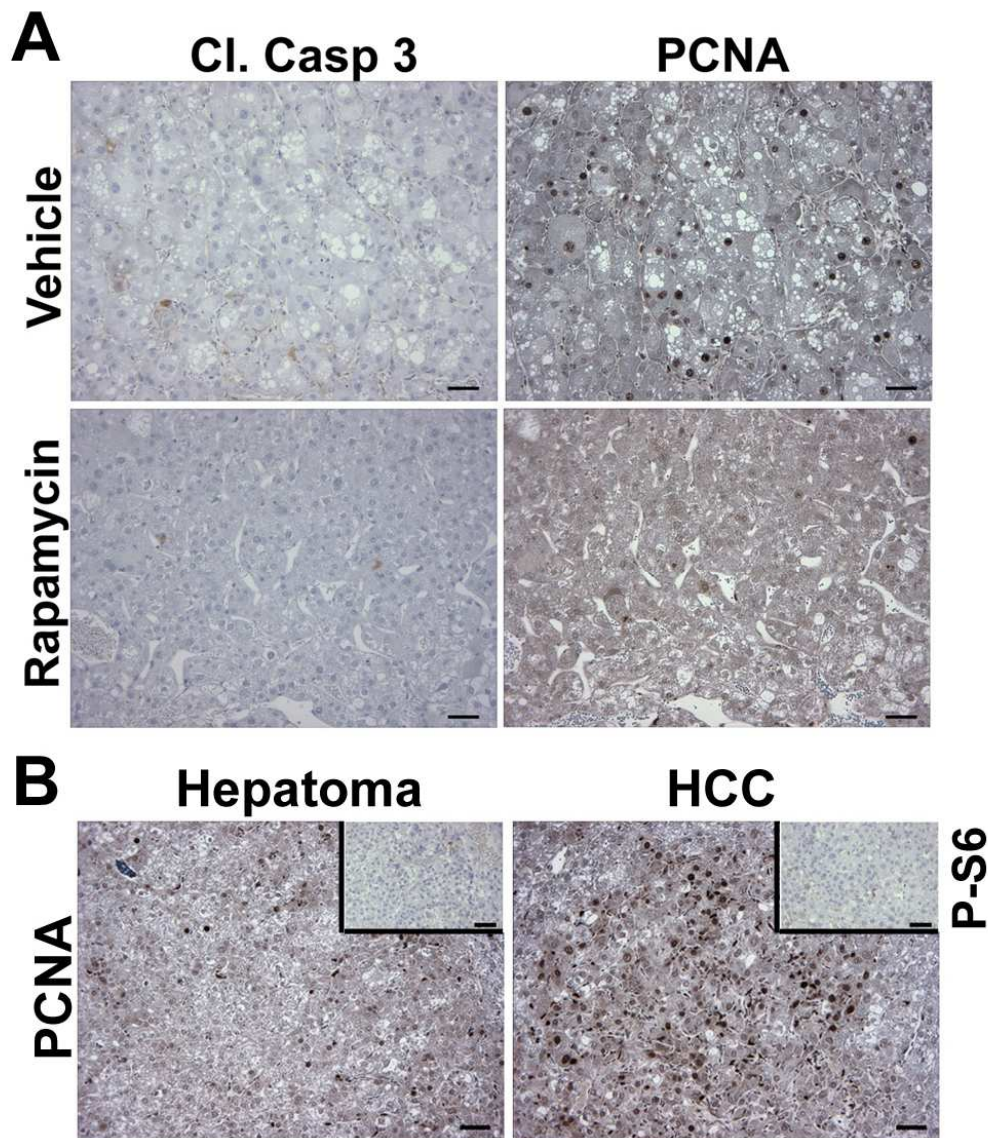
Supplemental Figure 5. Changes in *LTsc1KO* livers at 6 months of age before the appearance of tumors. (A) Immunoblot of liver lysates from *Tsc1^{fl/fl}* and *LTsc1KO* mice with the indicated antibodies. (B) Representative immunohistochemical staining of adjacent liver sections from *Tsc1^{fl/fl}* and *LTsc1KO* mice with F4/80 and PanCK antibodies showing overlapping areas of immune infiltration and progenitor cell expansion. The *Tsc1^{fl/fl}* and *LTsc1KO* livers show normal staining of F4/80 in Kupffer cells. Scale bars, 50 μ m (200X). (C) Quantitative RT-PCR analysis of the indicated genes in the livers of *Tsc1^{fl/fl}* and *LTsc1KO* mice. Data are presented as the mean

± SEM relative to *Tsc1^{fl/fl}* mice (n=4). *P<0.01 (*p53*) and *P<0.05 (*p21*) compared to *Tsc1^{fl/fl}* mice.



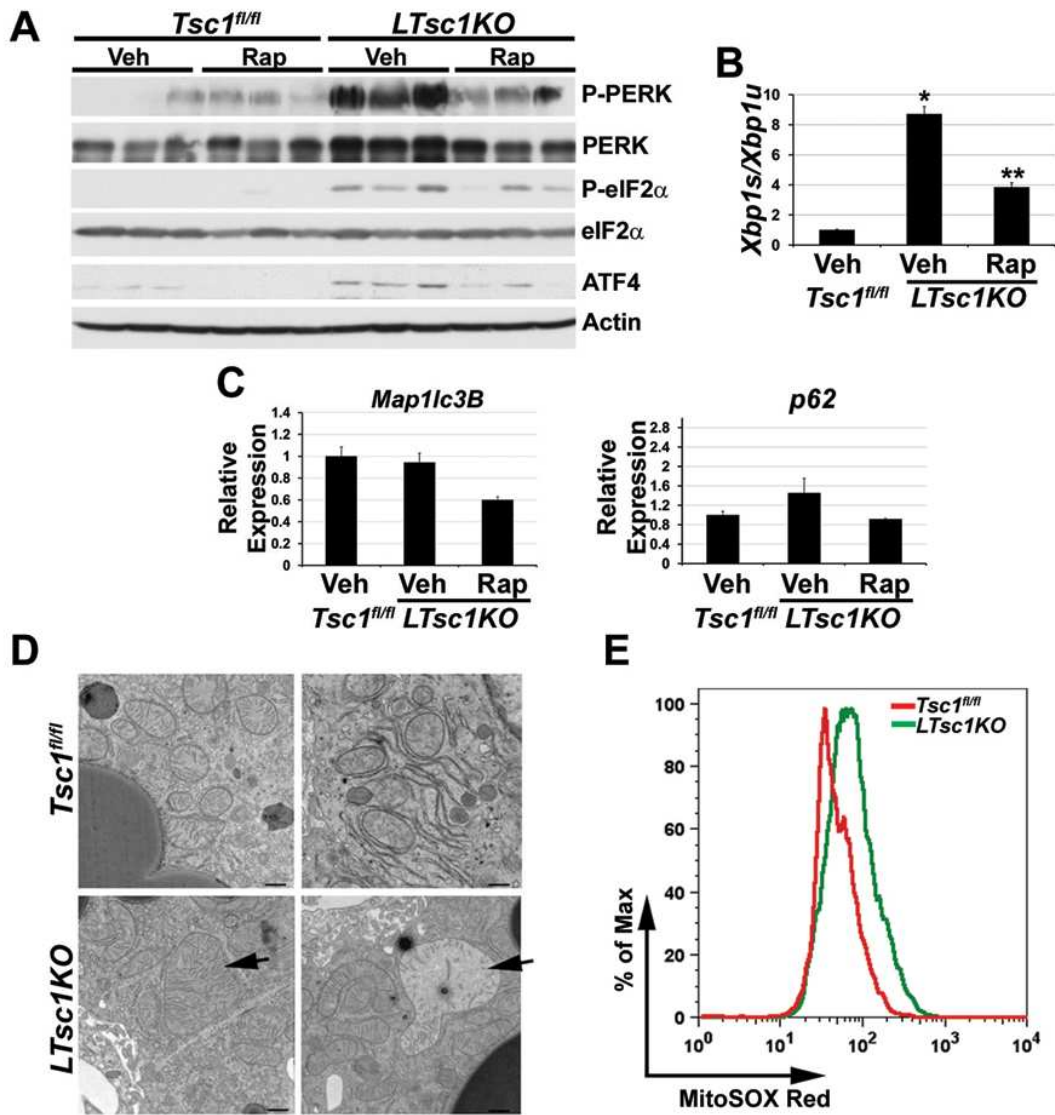
Supplemental Figure 6. Long-term rapamycin treatment of *LTsc1KO* mice decreases mTORC1 signaling, proliferation, apoptosis, inflammation, progenitor cell expansion, and DNA damage in the liver. As in Fig. 4, livers were harvested from mice at 10 months of age, following 5-months of treatment with vehicle or rapamycin (2 mg/kg, MWF), 48 hours after the final rapamycin dose. (A) Immunoblot of liver lysates from *Tsc1^{fl/fl}* and *LTsc1KO* mice treated with vehicle or rapamycin with the indicated antibodies. Phospho-specific antibody: S6 (Ser^{240/244}). (B) Representative images of immunohistochemical staining with the indicated antibodies in the non-

tumor regions of livers of *LTsc1KO* mice treated with vehicle or rapamycin. Scale bars, 50 μ m (200X).



Supplemental Figure 7. Cytostatic, but not cytotoxic, response of *LTsc1KO* liver tumors to rapamycin and inhibition of mTORC1 signaling by rapamycin in tumor regions resistant to rapamycin. As described in Fig. 5, mice were treated with vehicle or rapamycin (2 mg/kg, MWF) from 12 to 13 months of age, and livers were harvested 12 hours after the final rapamycin dose. (A) Representative immunohistochemical staining of the same tumor region for cleaved caspase-3 and PCNA in adjacent liver sections from *LTsc1KO* mice treated with vehicle or rapamycin. (B) Liver sections of a hepatoma and HCC from rapamycin-treated *LTsc1KO* mice, showing rapamycin-resistant proliferation (PCNA) in these tumor regions. Insets show low phospho-S6

(Ser^{240/244}) staining in the same tumor regions in adjacent sections. Scale bars, A and B, 50 μ m (200X).



Supplemental Figure 8. ER stress and defective mitochondria in *LTsc1KO* livers before the appearance of tumors. (**A**, **B**) Three female mice of each genotype at 3 months of age were treated with vehicle or rapamycin (5 mg/kg) for 4 consecutive days and then fasted overnight before harvesting the liver for isolation of protein and RNA for immunoblot analysis with the indicated antibodies (**A**) or qRT-PCR analysis of the given mRNA transcript (**B**). Phospho-specific antibodies: PERK (Thr⁹⁸⁰), eIF2 α (Ser⁵¹). Ratio of spliced to unspliced form of *Xbp1* mRNA abundance are presented as the mean \pm SEM relative to the vehicle-treated controls (n=3). *P<0.01 compared to vehicle-treated *Tsc1^{fl/fl}* mice, **P<0.05 compared to vehicle-treated

LTsc1KO mice. (C) qRT-PCR analysis of the indicated transcripts in livers of the mice described in Fig. 6A. Data are shown as the mean \pm SEM relative to the vehicle treated controls (n=3). No statistically significant differences. (D) Representative images from electron microscopy (EM) of the livers of *Tsc1^{fl/fl}* and *LTsc1KO* mice at 6 months of age (n=3). Mice were fasted overnight before processing of the livers for EM. Arrows indicate typical enlarged or dilated mitochondria of abnormal appearance in *LTsc1KO* livers. Scale bars, 500 nm (9300X). (E) Fluorescence-activated cell sorting (FACS) analysis of primary hepatocytes isolated from *Tsc1^{fl/fl}* and *LTsc1KO* mice, which were stained with MitoSOX Red to detect mitochondrial ROS.

Table S1. RT-PCR Primers Used in This Study

	Forward (5'-3')	Reverse (5'-3')
<i>Chop</i>	CCACCACACCTGAAAGCAGAA	AGGTGAAAGGCAGGGACTCA
<i>Erol</i>	TGGCTAGAAGGCCTCTGTGT	TGACCCCATTTCTTTTCCAG
<i>Map1LC3B</i>	CGCTTGCAGCTCAATGCTAAC	TGCCCATTCACCAGGAGGA
<i>SQSTM1</i>	ATGTGGAACATGGAGGGAAGA	GGAGTTCACCTGTAGATGGGT
<i>p53</i>	GCTTCTCCGAAGACTGGATG	GTCCATGCAGTGAGGTGATG
<i>p21</i>	CCTGGTGATGTCCGACCTG	CCATGAGCGCATCGCAATC
<i>Xbp1s</i>	GGTCTGCTGAGTCCGCAGCAGG	AGGCTTGGTGTATACATGG
<i>Xbp1u</i>	ACGGCCTTGTGGTTGAGAAC	TGTCCATTCCCAAGCGTGTT